

ENGINEERING RESEARCH INSTITUTE  
THE UNIVERSITY OF MICHIGAN  
ANN ARBOR

Final Report

STUDY OF THE HYPERSONIC LAMINAR BOUNDARY LAYER WITH DISSOCIATION

Part I

T. C. Adamson, Jr.  
P. M. Sherman  
J. A. Nicholls  
R. Dunlap

Project 2606

BELL AIRCRAFT CORPORATION  
BUFFALO, NEW YORK

September 1957



## TABLE OF CONTENTS

	Page.
LIST OF ILLUSTRATIONS	iii
ABSTRACT	iv
OBJECTIVE	iv
LIST OF SYMBOLS	v
INTRODUCTION	1
PERTURBATION OF BOUNDARY-LAYER EQUATIONS	1
CALCULATIONS ON THE EXISTENCE OF A BUFFER LAYER	12
SIMILARITY BETWEEN DISSOCIATED AND NONDISSOCIATED FLOWS	18
EXPERIMENTAL FACILITIES	21
REFERENCES	25

LIST OF ILLUSTRATIONS

	Page
Table I. Perfect Gas Specific Heats of Atomic and Molecular Oxygen and Molecular Nitrogen as a Function of Temperature	26
Fig. 1. Variation of time-ratio function with altitude with flight Mach number as parameter for flat plate of length L.	27
Fig. 2. Three-dimensional coordinates.	28
Fig. 3. Stagnation-point region between a detached shock and a blunt body.	28
Fig. 4. Variation of time-ratio function with altitude with flight Mach number as parameter for blunt-nose body with radius of curvature $R_{b0}$ .	29

ABSTRACT

The equations which hold for the quasi-two-component hypersonic boundary layer are perturbed slightly from the case of chemical equilibrium. The perturbation equations are derived up to and including second order, and some remarks about their solution and a possibly better formulation of the perturbation problem are made.

Functions which infer the existence or nonexistence of a buffer layer where no reaction occurs are plotted versus altitude with Mach number as a parameter for the stagnation-point region of a blunt body with a detached shock, and for the boundary layer behind a normal shock. These functions defined the so-called cross over altitude where the buffer layer ceases to exist, and reaction could occur along the wall. A method is proposed whereby an order of magnitude of the area covered by the wall reaction may be found.

Kuo's conditions for similarity are discussed, and some questions are raised concerning the validity of the assumptions made.

A discussion of the detonation tube and the electric arc drivers for hypersonic wind tunnels is presented. The electric arc is shown to give a better chance of achieving true similarity in the test section, used the energy levels necessary to obtain desired test-section conditions are discussed. Various methods of creating and storing the required energy are given.

OBJECTIVE

This study was made to improve understanding of equilibrium and nonequilibrium dissociation effects in the hypersonic laminar boundary layer.

LIST OF SYMBOLS

- $b$  = distance between nose of blunt body and shock along a stagnation streamline
- $C = \rho\mu/\rho_e\mu_e$
- $C_{P_i}$  = specific heat at constant pressure per unit mass of  $i$ th species
- $C_{P_i}^*$  = dimensionless specific heat,  $C_{P_i}/\bar{C}_{P_w}$
- $\bar{C}_p$  = specific heat of mixture,  $\bar{C}_p = \sum_i K_i C_{P_i}$
- $\bar{C}_p^*$  = dimensionless specific heat,  $\bar{C}_p/\bar{C}_{P_w}$
- $\mathcal{D}_{12}$  = binary diffusion coefficient for oxygen atoms and oxygen or nitrogen molecules
- $f$  = Blasius function
- $h_i$  = enthalpy per unit mass of  $i$ th species
- $h$  = enthalpy of mixture,  $h = \sum_i K_i h_i$ ,  $h_s = h + \frac{u^2}{2}$
- $\overline{\Delta H}_2$  = heat of reaction =  $h_1 - h_2$
- $\mathcal{K}_p$  = equilibrium coefficient in terms of partial pressures
- $l$  = characteristic chemical length,  $l = \sigma_e t_c$
- $Le$  = Lewis number,  $\bar{C}_p \rho \mathcal{D}_{12} / \lambda$
- $L$  = characteristic length in  $x$  direction
- $\mathcal{K}_i$  = rate at which molecules of  $i$ th species are formed per unit volume due to chemical reaction
- $M_i$  = molecular weight of  $i$ th species
- $\bar{M}$  = molecular weight of mixture
- $M$  = Mach number
- $\mathcal{P}$  = local pressure

LIST OF SYMBOLS (continued)

$P_r =$  Prandtl number,  $\bar{c}_p \mu / \lambda$

$Q =$  dimensionless heat of reaction,  $\Delta H_{12} / \bar{c}_{pw} T_w$

$\underline{q} =$  heat-flux vector

$r =$  radial distance in three-dimensional coordinates

$R_0 =$  universal gas constant

$R_b =$  radius of curvature of nose of blunt body

$R_s =$  radius of curvature of shock wave

$R_t =$  time ratio function,  $t_c / t_r$

$S_c =$  Schmidt number,  $\mu / \rho D_{12}$

$T =$  local temperature

$t_c =$  characteristic chemical time

$t_r =$  characteristic residence time

$u =$  mass average velocity in  $x$  direction in incompressible plane

$u_e =$  velocity external to boundary layer, in  $x$  direction

$v =$  mass average velocity in  $y$  direction in incompressible plane

$x =$  coordinate in incompressible plane

$y =$  coordinate in incompressible plane

$\alpha =$  angular displacement in three-dimensional coordinates

$\delta =$  boundary-layer thickness

$\eta =$  dimensionless coordinate,  $\eta = \frac{y}{z} \sqrt{\frac{u_e}{\nu_e x}}$

$\kappa_i =$  dimensionless mass concentration of species,  $\kappa_i = \rho_i / \rho$   
(Note 1  $\Rightarrow$   $O_2$  , 2  $\Rightarrow$   $O$  , 3  $\Rightarrow$   $N_2$  )

$\kappa = 1 - \kappa_2$

LIST OF SYMBOLS (concluded)

$\lambda$  = coefficient of thermal conductivity

$\mu$  = coefficient of dynamic viscosity

$\nu$  = kinematic viscosity,

$\rho_i$  = density of *i*th species

$\rho$  = density of mixture,  $\rho = \sum_i \rho_i$

$\xi$  = dimensionless coordinate,  $\xi = x/l$

$\theta$  = dimensionless temperature,  $\theta = T/T_w$

Subscripts

*e* = outer edge of boundary layer

*w* = surface of body

*0* = at  $x=0$



INTRODUCTION

This report covers the studies made as a continuation of the work covered in the first phase and reported in Technical Report No. 1. While it is entitled a final report, because it is the last report contemplated on the present contract, it does not cover the whole contract period, but simply the work done since the technical report.

The perturbation analysis was made using the equations which hold for the quasi-two-component system described in the first report (Ref. 1). Again, no attempt was made to account for a pressure gradient which would exist in the actual flow. However, in the buffer-layer calculation, a normal shock was taken into account in both the stagnation-point and boundary-layer cases.

The last section of the report contains the results of a study made to determine a suitable driver for a hypersonic wind tunnel wherein Mach number, total temperature, and altitude simulation could be obtained.

PERTURBATION OF BOUNDARY-LAYER EQUATIONS

The equations which hold for a quasi-two component boundary-layer in the plane are as follows (Eqs. 50, Ref. 1).

$$\begin{aligned}
 a) \quad & \frac{\partial}{\partial \eta} \left( \frac{c}{\epsilon} \frac{\partial \kappa}{\partial \eta} \right) + f \frac{\partial \kappa}{\partial \eta} = x \left[ \frac{4}{u_e} w + 2 \left\{ \frac{\partial f}{\partial \eta} \frac{\partial \kappa}{\partial x} - \frac{\partial f}{\partial x} \frac{\partial \kappa}{\partial \eta} \right\} \right] \\
 b) \quad & \frac{\partial}{\partial \eta} \left( \frac{c}{\epsilon} \frac{\kappa_3}{\kappa} \frac{\partial \kappa}{\partial \eta} \right) + f \frac{\partial \kappa_3}{\partial \eta} = 2x \left\{ \frac{\partial f}{\partial \eta} \frac{\partial \kappa_3}{\partial x} - \frac{\partial f}{\partial x} \frac{\partial \kappa_3}{\partial \eta} \right\} \\
 c) \quad & \frac{\partial}{\partial \eta} \left( c \frac{\partial^2 f}{\partial \eta^2} \right) + f \frac{\partial^2 f}{\partial \eta^2} = 2x \left\{ \frac{\partial f}{\partial \eta} \frac{\partial^2 f}{\partial x \partial \eta} - \frac{\partial f}{\partial x} \frac{\partial^2 f}{\partial \eta^2} \right\} \\
 d) \quad & \frac{\partial}{\partial \eta} \left( \frac{c}{\rho} \left[ \frac{\partial h_s}{\partial \eta} - (1-P) \frac{u_e^2}{8} \frac{\partial}{\partial \eta} \left( \left( \frac{\partial f}{\partial \eta} \right)^2 \right) - (1-\frac{P}{\epsilon}) \sum_i h_i \frac{\partial \kappa_i}{\partial \eta} \right] \right) + f \frac{\partial h_s}{\partial \eta} = \\
 & = 2x \left\{ \frac{\partial f}{\partial \eta} \frac{\partial h_s}{\partial x} - \frac{\partial f}{\partial x} \frac{\partial h_s}{\partial \eta} \right\}
 \end{aligned} \tag{1}$$

where the symbols are defined on page iv. In Eq. (1a),  $w$  represents the net amount of oxygen atoms being formed by the dissociation and recombination of oxygen, and is a function of pressure, temperature, and concentration. Thus,

$$w = - (2k_{re}) 2 \left( \frac{P}{R_0} \right)^2 \frac{1}{T^2} \left[ \frac{K_2^2}{K_2+1} - \frac{K_P}{4P} (1-K_2-K_3) \right] \quad (2)$$

$$= - 1.54 \times 10^{10} \left( \frac{P}{R_0} \right)^2 T^{-1/2} \left[ \frac{(1-K)^2}{2-K} - \frac{K_P}{4P} (K-K_3) \right]$$

where

$$K_P = \text{EXP.} \left( 15.8 - \frac{60000}{T} \right)$$

In Eqs. (1), the dependent variables have not been assumed functions of  $\eta$  alone, as is usually done in boundary-layer theory, since this is a valid assumption only if chemical equilibrium exists, or if no reaction occurs at all, for both of which cases,  $w \equiv 0$ .\* It is clear that if  $w \neq 0$ , an explicit  $X$  occurs in Eq. (1a), invalidating an assumption that  $K = K(\eta)$ , for instance. While the great majority of analyses have dealt with the case of chemical equilibrium, it is of interest to investigate the case of nonequilibrium flow, even if only to investigate what trends develop as the reaction develops in such a way that conditions are only slightly different from those at equilibrium. From such a perturbation analysis one might hope to find the initial effects of nonequilibrium on the heat transfer and skin friction.

Before carrying out the perturbation analysis, some remarks about the value of  $C = \rho u / \rho_e u_e$  and its effect on the velocity distribution should be made. First, as Probstein<sup>2</sup> has pointed out, variations in  $C$  cause little variation in  $f$ , the Blasius function, and since the variations of  $C$  from its equilibrium value are small, the effect on  $f$  of a perturbation in  $C$  must be negligible. Consideration of the other equations indicates that since  $C$  enters these equations in a manner exactly similar to the Blasius equation, Probstein's remarks should hold for them also, and hence any effects of a perturbation in  $C$  must be quite small and will be assumed negligible. The results of these arguments are, then, that it is assumed that  $C$  can be calculated from chemical equilibrium considerations. It is then a function only of  $\eta$ , and hence  $f$ , the Blasius function, is a function only of  $\eta$  again.

\*Fay and Riddell (see Ref. 10) consider  $w = 0$  only for the case of frozen flow, so that  $w$ , in the case of equilibrium flow, can be calculated from the species conservation equation, even though, by the classical definition, chemical equilibrium is that condition where there is no net time rate of production of any species, and hence  $w \equiv 0$ .

Since the reaction term,  $w$ , is written in terms of the temperature, rather than the total enthalpy, it is more appropriate to write the energy equation in terms of the temperature. Equation (47b) of Ref. 1 may be used, then, after transforming variables to  $\eta$  and  $X$ . With the above-mentioned assumptions on  $C$  and  $f$ , the equations then may be written as follows:

$$\begin{aligned}
 a) \quad & \frac{\partial}{\partial \eta} \left( \frac{C}{S_c} \frac{\partial K}{\partial \eta} \right) + f \frac{\partial K}{\partial \eta} - 2X f' \frac{\partial K}{\partial X} = \frac{4}{\sigma_e} X w \\
 b) \quad & \frac{\partial}{\partial \eta} \left( \frac{C}{S_c} \frac{K_3}{K} \frac{\partial K}{\partial \eta} \right) + f \frac{\partial K_3}{\partial \eta} - 2X f' \frac{\partial K_3}{\partial X} = 0 \\
 c) \quad & \frac{d}{d\eta} (C f'') + f f'' = 0 \\
 d) \quad & \frac{\partial}{\partial \eta} \left( \frac{C}{Pr} \bar{C}_p \frac{\partial T}{\partial \eta} \right) + f \bar{C}_p \frac{\partial T}{\partial \eta} - 2X \bar{C}_p f' \frac{\partial T}{\partial X} = \frac{-4}{\sigma_e} X \bar{\Delta H}_{12} w \\
 & - \frac{C U_e^2}{4} (f'')^2 + \frac{C}{S_c} \sum_{i=1}^3 C_p \frac{\partial K_i}{\partial \eta} \frac{\partial T}{\partial \eta}
 \end{aligned} \tag{3}$$

In the above equations,  $Pr$  and  $S_c$ , the Prandtl number and Schmidt number, respectively, are not necessarily constant. However, the change in Prandtl number, for example, has been shown by Hansen<sup>3</sup> to be very small, and these changes are neglected, so that in the remainder of this report both  $Pr$  and  $S_c$  are assumed constant. Also  $\bar{C}_p$ , being a function of temperature and pressure through the concentration, is assumed to be that  $\bar{C}_p$  calculated using chemical equilibrium, with no perturbation effects. Finally,  $\bar{\Delta H}_{12} = h_1 - h_2$  is the heat of dissociation, and actually varies with temperature. However, it is assumed constant.

Next,  $X$  is made dimensionless by dividing by  $l$ , a characteristic length. In view of the fact that the dissociation is the dominant feature of the present study, a characteristic chemical length is chosen in the same manner as in problems of combustion in flowing systems.<sup>4</sup> This is done in the following manner. The chemical length,  $l$ , may be computed from a characteristic velocity and a characteristic chemical time. Then,

$$l = \sigma_e t_c \tag{4}$$

where  $\sigma_e$  is chosen as the characteristic velocity. Next,  $t_c$  is chosen as the time associated with either the dissociation or recombination reaction at equilibrium (where the two are equal) at the maximum temperature reached in the equilibrium boundary layer. Thus, it is approximately the minimum time for the dissociation or recombination to occur, since the maximum reaction rate occurs

close to the maximum temperature. Actually, the maximum rate depends on both the concentration and the temperature, but the effects of temperature are so pronounced, compared to the effects of concentration, that the maximum rate occurs at a point near the maximum temperature. The maximum reaction rate, or minimum characteristic time, is chosen so that  $l$  may be interpreted as a maximum length, and hence used as an order-of-magnitude gauge in the perturbation analysis.

Considering the units of  $Pu$  in Ref. 1, it is clear that  $w$ , as defined, is already in the units of 1/sec, so that  $t_c$  is

$$\begin{aligned}
 t_c &= \frac{1}{w_{x,f}} = 0.65 \times 10^{-10} \left(\frac{R_0}{P}\right)^2 \frac{1}{(T_{max}^{(0)})^{1/2}} \left[ \frac{2 - K^{(0)}}{1 - K^{(0)}} \right]_{T_{max}^{(0)}}^{-1} \\
 &= 0.65 \times 10^{-10} \frac{1}{(T_{max}^{(0)})^{1/2}} 4P \left[ \chi_{12}^{(0)} (K^{(0)} - K_3^{(0)}) \right]^{-1}
 \end{aligned} \tag{5}$$

where the superscript (0) indicates the equilibrium values. From the above definition, it is seen that  $t_c$  is a constant for any given set of external conditions, but must be calculated for each set.

The dimensionless  $x$  variable,  $\xi$ , is then defined as follows:

$$\xi = x/l \tag{6}$$

Finally, define a dimensionless temperature, specific heats, and heat of dissociation.

$$\begin{aligned}
 a) \quad \theta &= T/T_w \\
 b) \quad C_p^* &= \bar{C}_p / \bar{C}_{p_w} \\
 c) \quad C_{p_i}^* &= C_{p_i} / \bar{C}_{p_w} \\
 d) \quad q &= \frac{\bar{\Delta H}_{12}}{\bar{C}_{p_w} T_w}
 \end{aligned} \tag{7}$$

With the above definitions, Eqs. (3) may be written as follows:

$$a) \frac{\partial}{\partial \eta} \left( \frac{c}{s_c} \frac{\partial \kappa}{\partial \eta} \right) + f \frac{\partial \kappa}{\partial \eta} - 2f' \zeta \frac{\partial \kappa}{\partial \zeta} = 4 \zeta (w t_c)$$

$$b) \frac{\partial}{\partial \eta} \left( \frac{c}{s_c} \frac{\kappa_3}{\kappa} \frac{\partial \kappa}{\partial \eta} \right) + f \frac{\partial \kappa_3}{\partial \eta} - 2f' \zeta \frac{\partial \kappa_3}{\partial \zeta} = 0$$

$$c) (c f'')' + f f'' = 0 \tag{8}$$

$$d) \frac{\partial}{\partial \eta} \left( \frac{c}{R} C_P^* \frac{\partial \theta}{\partial \eta} \right) + f C_P^* \frac{\partial \theta}{\partial \eta} - 2f' \zeta C_P^* \frac{\partial \theta}{\partial \zeta} = -4 \zeta Q(w t_c)$$

$$- \frac{c}{4} \frac{U_e^2}{C_P^* T_w} (f'')^2 + \frac{c}{s_c} \sum_{i=1}^3 C_{P_i}^* \frac{\partial \kappa_i}{\partial \eta} \frac{\partial \theta}{\partial \eta}$$

Consideration of Eqs. (8) indicates that the appropriate expression for  $\theta$ ,  $\kappa$ , and  $\kappa_3$ , when  $\zeta = \frac{x}{l} \ll 1$ , are as follows:

$$\theta = \theta^{(0)}(\eta) + \zeta \theta^{(1)}(\eta) + \zeta^2 \theta^{(2)}(\eta) + \dots$$

$$\kappa = \kappa^{(0)}(\eta) + \zeta \kappa^{(1)}(\eta) + \zeta^2 \kappa^{(2)}(\eta) + \dots \tag{9}$$

$$\kappa_3 = \kappa_3^{(0)}(\eta) + \zeta \kappa_3^{(1)}(\eta) + \zeta^2 \kappa_3^{(2)}(\eta) + \dots$$

In these relations, the zero'th-order terms are functions of  $\eta$  alone since they refer to the case of chemical equilibrium ( $w \equiv 0$ ). The reaction rate term,  $w$ , may be expanded first. In order to expand  $w$  in terms of the above variables, Hirschfelder's approximation for  $\mathcal{K}_P$  may be used, as indicated in Ref. 1. Thus,

$$\begin{aligned} \mathcal{K}_P &\cong \text{EXP} \left( 15.8 - \frac{60000}{T} \right) \\ &= \text{EXP}(15.8) \text{EXP} \left( -\frac{60000}{T_w} \frac{1}{\theta} \right) \end{aligned} \tag{10}$$

Now,

$$\frac{1}{\theta} = \frac{1}{\theta^{(0)}(1 + \zeta \theta^{(1)}/\theta^{(0)})} \cong \frac{1}{\theta^{(0)}} \left( 1 - \zeta \frac{\theta^{(1)}}{\theta^{(0)}} \right)$$

so that

$$\begin{aligned} \kappa_p &= \exp(15.8) \exp\left(-\frac{60000}{T_w} \frac{1}{\theta^{(0)}}\right) \left(1 + 3 \frac{60000}{T_w} \frac{\theta^{(1)}}{\theta^{(0)}}\right) \\ &= \kappa_p^{(0)} \left(1 + 3 \frac{60000}{T_w} \frac{\theta^{(1)}}{\theta^{(0)}}\right) \end{aligned} \quad (11)$$

where

$$\kappa_p^{(0)} = \exp\left(15.8 - \frac{60000}{T_w} \frac{1}{\theta^{(0)}}\right) \quad (12)$$

With the above expansion for  $\kappa_p$ ,  $W$  may be expanded to give

$$\begin{aligned} W &= -1.54 \times 10^{10} \left(\frac{P}{R_0}\right)^2 \sqrt{T_w} (\theta^{(0)} + 3 \theta^{(1)})^{1/2} \left[ \frac{(1 - (\kappa^{(0)} + 3\kappa^{(1)}))^2}{(2 - (\kappa^{(0)} + 3\kappa^{(1)}))} - \right. \\ &\quad \left. - \frac{\kappa_p^{(0)} (1 + 3 \frac{60000}{T_w} \frac{\theta^{(1)}}{\theta^{(0)}})}{4P} (\kappa^{(0)} + 3\kappa^{(1)} - (\kappa_3^{(0)} + 3\kappa_3^{(1)})) \right] \\ &= 1.54 \times 10^{10} \left(\frac{P}{R_0}\right)^2 \sqrt{T_w} (\theta^{(0)})^{1/2} \left[ \frac{\kappa_p^{(0)} (\kappa^{(0)} - \kappa_3^{(0)})}{4P} \right] \left[ \frac{\theta^{(1)}}{\theta^{(0)}} \frac{60000}{T_w} + \right. \\ &\quad \left. + \kappa^{(1)} \left( \frac{1}{\kappa^{(0)} - \kappa_3^{(0)}} + \frac{2}{1 - \kappa^{(0)}} - \frac{1}{2 - \kappa^{(0)}} \right) - \kappa_3^{(1)} \frac{1}{\kappa^{(0)} - \kappa_3^{(0)}} \right] \end{aligned}$$

since  $\frac{(1 - \kappa^{(0)})^2}{(2 - \kappa^{(0)})} = \frac{\kappa_p^{(0)}}{4P} (\kappa^{(0)} - \kappa_3^{(0)})$ , due to chemical equilibrium.

Next, introducing  $t_c$ , one obtains the following relationship:

$$\begin{aligned} t_c W &= \left(\frac{\theta^{(0)}}{\theta_m^{(0)}}\right)^{1/2} \frac{\kappa_p^{(0)} (\kappa^{(0)} - \kappa_3^{(0)})}{\left[ \kappa_p^{(0)} (\kappa^{(0)} - \kappa_3^{(0)}) \right]_{T=T_{max}}} \left[ \frac{\theta^{(1)}}{\theta^{(0)}} \frac{60000}{T_w} + \right. \\ &\quad \left. + \kappa^{(1)} \left( \frac{1}{\kappa^{(0)} - \kappa_3^{(0)}} + \frac{2}{1 - \kappa^{(0)}} - \frac{1}{2 - \kappa^{(0)}} \right) - \kappa_3^{(1)} \frac{1}{\kappa^{(0)} - \kappa_3^{(0)}} \right] \end{aligned} \quad (13)$$

Finally, the following symbols are defined:

$$a) S(\eta) = \frac{\rho_p^{(0)} (K^{(0)} - K_3^{(0)})}{[\rho_p^{(0)} (K^{(0)} - K_3^{(0)})]_{T=T_{max}^{(0)}}}$$

$$b) \theta_a = \frac{60000}{T_w} \quad (14)$$

$$c) F(\eta) = \frac{1}{K^{(0)} - K_3^{(0)}} + \frac{2}{1 - K^{(0)}} - \frac{1}{2 - K^{(0)}}$$

$$d) G(\eta) = \frac{1}{K^{(0)} - K_3^{(0)}}$$

Then,

$$t_c w = \left( \frac{\theta^{(0)}}{\theta_m^{(0)}} \right)^{1/2} S(\eta) \left[ \frac{\theta_a}{\theta^{(0)}} \frac{\theta^{(1)}}{\theta^{(0)}} + F(\eta) K^{(1)} - G(\eta) K_3^{(1)} \right] \zeta \quad (15)$$

Next, if Eqs. (15) and (9) are substituted into Eqs. (8a) through (8d), and the coefficients of like powers of  $\zeta$  are equated, there result the zero'th-, first-, and second-, etc. order perturbation equations. These equations are given below.

Zero'th-order equations:

$$a) \frac{d}{d\eta} \left( \frac{c}{s_c} \frac{dK^{(0)}}{d\eta} \right) + f \frac{dK^{(0)}}{d\eta} = 0$$

$$b) \frac{d}{d\eta} \left( \frac{c}{s_c} \frac{K_3^{(0)}}{K^{(0)}} \frac{dK^{(0)}}{d\eta} \right) + f \frac{dK_3^{(0)}}{d\eta} = 0 \quad (16)$$

$$c) \frac{d}{d\eta} \left( \frac{c}{R} C_p^* \frac{d\theta^{(0)}}{d\eta} \right) + f C_p^* \frac{d\theta^{(0)}}{d\eta} = - \frac{c}{4} \frac{\sigma_e^2}{C_p T_w} (f''')^2 + \frac{c}{s_c} (C_{p1}^* - C_{p2}^*) \frac{d\theta^{(0)}}{d\eta} \frac{dK^{(0)}}{d\eta}$$

First-order equations:

$$\begin{aligned}
 \text{a) } & \frac{d}{d\eta} \left( \frac{C}{S_c} \frac{dK^{(1)}}{d\eta} \right) + f \frac{dK^{(1)}}{d\eta} - 2f'K^{(1)} = 0 \\
 \text{b) } & \frac{d}{d\eta} \left( \frac{C}{S_c} \frac{K_3^{(0)}}{K^{(0)}} \left\{ \left( \frac{K_3^{(1)}}{K_3^{(0)}} - \frac{K^{(1)}}{K^{(0)}} \right) \frac{dK^{(0)}}{d\eta} + \frac{dK^{(1)}}{d\eta} \right\} \right) + f \frac{dK_3^{(1)}}{d\eta} - 2f'K_3^{(1)} = 0 \\
 \text{c) } & \frac{d}{d\eta} \left( \frac{C}{R} C_p^* \frac{d\theta^{(1)}}{d\eta} \right) + f C_p^* \frac{d\theta^{(1)}}{d\eta} - 2f' C_p^* \theta^{(1)} = \\
 & = \frac{C}{S_c} (C_{P_1}^* - C_{P_2}^*) \left( \frac{dK^{(1)}}{d\eta} \frac{d\theta^{(0)}}{d\eta} + \frac{dK^{(0)}}{d\eta} \frac{d\theta^{(1)}}{d\eta} \right)
 \end{aligned} \tag{17}$$

Second-order equations:

$$\begin{aligned}
 \text{a) } & \frac{d}{d\eta} \left( \frac{C}{S_c} \frac{dK^{(2)}}{d\eta} \right) + f \frac{dK^{(2)}}{d\eta} - 4f'K^{(2)} = 4 \left( \frac{\theta^{(0)}}{\theta_m^{(0)}} \right)^{1/2} \int \frac{\theta_a \theta^{(1)}}{\theta^{(0)} \theta^{(0)}} + FK^{(1)} - GK_3^{(1)} \\
 \text{b) } & \frac{d}{d\eta} \left( \frac{C}{S_c} \frac{K_3^{(0)}}{K^{(0)}} \left\{ \left( \frac{K_3^{(2)}}{K_3^{(0)}} - \frac{K^{(2)}}{K^{(0)}} \frac{K_3^{(1)}}{K_3^{(0)}} + \left( \frac{K^{(1)}}{K^{(0)}} \right)^2 - \frac{K^{(2)}}{K^{(0)}} \right) \frac{dK^{(0)}}{d\eta} + \left( \frac{K_3^{(1)}}{K_3^{(0)}} - \frac{K^{(1)}}{K^{(0)}} \right) \frac{dK^{(0)}}{d\eta} + \frac{dK^{(2)}}{d\eta} \right\} \right) + f \frac{dK_3^{(2)}}{d\eta} - 4f'K_3^{(2)} = 0 \\
 \text{c) } & \frac{d}{d\eta} \left( \frac{C}{R} C_p^* \frac{d\theta^{(2)}}{d\eta} \right) + f C_p^* \frac{d\theta^{(2)}}{d\eta} - 4C_p^* f' \theta^{(2)} = \\
 & = -4Q \left( \frac{\theta^{(0)}}{\theta_m^{(0)}} \right)^{1/2} \int \frac{\theta_a \theta^{(1)}}{\theta^{(0)} \theta^{(0)}} + FK^{(1)} - GK_3^{(1)} + \frac{C}{S_c} (C_{P_1}^* - C_{P_2}^*) \left( \frac{dK^{(2)}}{d\eta} \frac{d\theta^{(0)}}{d\eta} + \frac{dK^{(0)}}{d\eta} \frac{d\theta^{(2)}}{d\eta} + \frac{dK^{(1)}}{d\eta} \frac{d\theta^{(1)}}{d\eta} + \frac{dK^{(1)}}{d\eta} \frac{d\theta^{(2)}}{d\eta} \right)
 \end{aligned} \tag{18}$$

The boundary conditions for the above equations are as follows:

$$\begin{aligned}
 @ \eta = 0 & \quad K^{(0)} = K_w & \quad K^{(1)} = K^{(2)} = 0 \\
 & \quad K_3^{(0)} = K_{3w} & \quad K_3^{(1)} = K_3^{(2)} = 0 \\
 & \quad \theta^{(0)} = \theta_w & \quad \theta^{(1)} = \theta^{(2)} = 0 \\
 & \quad f = f' = 0
 \end{aligned} \tag{19}$$



$$\begin{aligned}
 @ \eta = \infty \quad & K^{(0)} = K_e & K^{(1)} = K^{(2)} = 0 \\
 & K_3^{(0)} = K_{3e} & K_3^{(1)} = K_3^{(2)} = 0 \\
 & \theta^{(0)} = \theta_e & \theta^{(1)} = \theta^{(2)} = 0 \\
 & f' = 2
 \end{aligned} \tag{20}$$

Here  $K_w$  is the equilibrium value of the concentration at the given wall temperature if the wall is considered to have no poisoning effect on the reaction. This is the assumption made here since no better information to the contrary exists at the present time for the materials under consideration.

It should be noted that in Eqs. (16), (17), and (18), the reaction terms do not appear until the second-order Eqs. (18). The reason for this is that  $w^{(0)} = 0$  from equilibrium, so that no first-order reaction term exists. Although this result implies that a possible solution to the first-order equation is  $K^{(1)} = K_3^{(1)} = \theta^{(1)} = 0$ , it is clear from the expansion of the reaction rate that  $K^{(1)} = K_3^{(1)} = \theta^{(1)} = 0$  is true only if  $w \equiv 0$ , that is, if there is complete equilibrium, or no reaction at all. Hence there is an implicit relationship between the first-order quantities, and the forcing function (reaction term).

While no solution was found for the above set of equations, some remarks may be made about their solutions. First the energy equation may be made more similar to the species continuity equations by neglecting the term  $C_p^* - C_B^*$ . Table I shows the values of  $C_{P_{O_2}}$ ,  $C_{P_O}$ , and  $C_{P_{N_2}}$  at various temperatures. Since it has already been assumed that  $C_{P_{O_2}} \cong C_{P_{N_2}}$ , and since the difference between  $C_{P_O}$  and  $C_{P_{O_2}}$  is less than that between  $C_{P_{O_2}}$  and  $C_{P_{N_2}}$  in most cases, little additional error is introduced. The result of this assumption is that  $C_P = C_B = C_B^* = C_P$  and hence  $\bar{C}_P = C_P$  and  $C_p^* = 1$ .

The zero'th-order energy equation is now the equation used in the calculation of the equilibrium boundary layer, and hence it is assumed solved. However, the zero'th-order species continuity equations have little meaning in this case, since the equilibrium concentrations are computed not from the first two Eqs. (16) but from the chemical equation which expresses equilibrium relationship for the given reaction at the given temperature and pressure. Furthermore, the rates of reaction are usually assumed to be so fast that any small change in concentration from equilibrium is instantaneously changed so that equilibrium again exists. Hence the zero'th-order concentration equations give only a means of calculating the amount of mass being diffused and convected across any given plane, with the proviso that any change from chemical equilibrium is instantly counteracted by the reaction. However, these equations must be satisfied in general, since they represent the conservation of mass for the indicated species.

With the above remarks in mind a possible similarity between  $\kappa$  and  $\kappa_3$  is proposed. Consideration of Eqs. (16a) and (16b) and the boundary conditions on  $\kappa^{(0)}$  and  $\kappa_3^{(0)}$  show that so long as the temperature at the wall and at the boundary-layer edge are such that the assumption of local equilibrium means that  $\kappa_2 = 0$ , or that  $\kappa = 1$ , then a possible solution to the equation for  $\kappa_3^{(0)}$  is

$$\kappa_3^{(0)} = a \kappa^{(0)}. \quad (21)$$

where  $a$  is a constant. Equation (21) then satisfies the equation and boundary conditions for  $\kappa_3^{(0)}$ , translating them into the corresponding equations and boundary conditions for  $\kappa^{(0)}$ .

The above argument can be made for  $\kappa_3^{(1)}$ , also. Thus, if

$$\kappa_3^{(1)} = a \kappa^{(1)} = \frac{\kappa_3^{(1)}}{\kappa^{(1)}} \quad (22)$$

then  $\frac{\kappa_3^{(1)}}{\kappa_3^{(0)}} = \frac{\kappa^{(1)}}{\kappa^{(0)}}$  and Eq. (17b) becomes

$$\frac{d}{d\eta} \left( \frac{c}{S_c} a \frac{d\kappa^{(1)}}{d\eta} \right) + a f \frac{d\kappa^{(1)}}{d\eta} - 2 f' a \kappa^{(1)} = 0$$

which is identical to Eq. (17a) multiplied by  $a$ . Furthermore, since the boundary conditions are that  $\kappa_3^{(0)} = \kappa^{(0)} = 0$  at the outer edge and wall boundaries, the boundary conditions are satisfied. However, at this point it is not clear what this type of solution means. Since the equation for  $\kappa^{(0)}$  is essentially meaningless insofar as calculation of the actual values for  $\kappa^{(0)}$  is concerned, it seems that one must use the values of  $\kappa^{(0)}$  which are computed from chemical equilibrium, in the first- and second-order equations. In that case, the above method of solution is not correct. On the other hand, the zero'th-order equations must hold, and, thus the equation for  $\kappa^{(0)}$  must be satisfied, instantaneously. In reality, this problem must be faced in any equilibrium calculations. That is, the conservation equations for each species still hold whether chemical equilibrium exists or not. However, they are usually dismissed with the assumption that the equilibrium reaction rates are infinitely fast, as discussed above. The important point is the following: Can the zero'th-order equations (equilibrium conservation equations) be used to represent the concentrations in the first-order equations, again with the proviso that any change from chemical equilibrium is instantly counteracted by the reaction? This is the only way that the above solution could be explained, and it seems a very weak explanation, so that probably a much more complicated relationship exists between  $\kappa^{(0)}$  and  $\kappa_3^{(0)}$ .

No general solution was found for the type of equation represented by Eq. (17a). Since Eq. (17a) is essentially the homogeneous part of the second-

order Eqs. (18), it is evident that if a solution of (17a) could be found, integral solutions for Eqs. (18) could be written, and the numerical work performed very quickly. However, the only known solutions for an equation of the (17a) type is for the case where  $f' = C_1$ , and  $f = C_1 \eta$ , where  $C_1$  is a constant. The only place this could possibly have any meaning in the boundary layer would be at the outer edge where  $f' \cong 2$ , and this is not the interesting region.

Although no formal solution for  $\kappa^{(1)}$ ,  $\kappa_3^{(1)}$ , etc., was found, the heat-transfer relation may be written in terms of the perturbation quantities. In general, the heat-flux vector is (see Ref. 1):

$$\begin{aligned} q_y &= -\lambda \frac{\partial T}{\partial y_0} + \sum_i \rho_i v_i h_i \\ &= -\lambda T_w \frac{\partial \theta}{\partial y_0} - \rho \alpha D_{12} \sum_i h_i \frac{\partial \kappa_i}{\partial y_0} \end{aligned} \quad (23)$$

Also, in view of the assumptions made about components one and three,

$$\begin{aligned} \sum_i h_i \frac{\partial \kappa_i}{\partial y_0} &= h_1 \frac{\partial (\kappa_1 + \kappa_3)}{\partial y_0} + h_2 \frac{\partial \kappa_2}{\partial y_0} \\ &= (h_1 - h_2) \frac{\partial \kappa}{\partial y_0} \end{aligned} \quad (24)$$

where  $\overline{\Delta H_{12}} = h_1 - h_2$  has already been assumed constant. In terms of  $\eta$ , the boundary-layer variable, the heat flux at the wall is, then,

$$q_{yw} = -\frac{\lambda_w T_w}{2} \left( \frac{U_e}{v_{ex}} \right)^{1/2} \left[ \frac{\partial \theta}{\partial \eta} + \frac{\bar{c}_p \rho \alpha D_{12}}{\lambda} \frac{\overline{\Delta H_{12}}}{c_{p_w} T_w} \frac{\partial \kappa}{\partial \eta} \right]_{wall} \quad (25)$$

where  $\bar{c}_p \rho \alpha D_{12} / \lambda = Pr / Sc = Le$  is the Lewis number, and is constant. Finally, then, in terms of the perturbation quantities, one can write

$$\begin{aligned} q_{yw} &= -\frac{\lambda_w T_w}{2} \left( \frac{U_e}{v_{ex}} \right)^{1/2} \left[ \left\{ \frac{d\theta^{(1)}}{d\eta} + Le \frac{\overline{\Delta H_{12}}}{c_{p_w} T_w} \frac{d\kappa^{(1)}}{d\eta} \right\}_{wall} + \right. \\ &\quad \left. + \left\{ \frac{d\theta^{(2)}}{d\eta} + Le \frac{\overline{\Delta H_{12}}}{c_{p_w} T_w} \frac{d\kappa^{(2)}}{d\eta} \right\} + \dots \right] \end{aligned} \quad (26)$$

Again, the zero'th-order terms are those which would exist in the usual calculation of the heat transfer at the wall in the equilibrium boundary layer. It should be noted that since the wall temperature is usually too-low to support the dissociation reaction then usually  $dk^0/d\eta=0$ , until the pressure becomes so low (high altitude) that there is appreciable nonequilibrium reaction even at the lower temperatures. This, incidentally, is one of the reasons why at low altitude the equilibrium boundary-layer heat transfer is almost identically equal to the heat transfer in a boundary layer with no dissociation. However, at higher altitudes, where reaction may proceed much slower, equilibrium may not be reached as fast, and a concentration gradient may exist.

To conclude these remarks on the perturbation analysis, it must be said that the present setup does not seem to simplify the problem as was desired. The questions raised by the very fact that the zero'th-order equations are for a flow at chemical equilibrium still exist. First, what is the meaning of the zero'th-order equation, and secondly, what is the physical meaning behind the fact that the reaction rates do not affect the first-order equations? More thought should be given to both the present setup and also to a different perturbation scheme which might bring the physical concepts into better focus. For example, one might prescribe a small quantity which was better defined than  $\xi$ . In the present case,  $\xi = x/\ell$ , where  $\ell$  is a characteristic chemical length based on  $\bar{v}_e$  and a characteristic chemical time. The chemical time was based on either the dissociation or recombination reaction at equilibrium (they being equal) at the maximum boundary-layer temperature. Thus, the  $\ell$  used was a minimum, so it was a conservative length. However,  $\xi$  small means only that  $x$ , the physical distance, is small compared to an equilibrium chemical length, or that  $\ell$  is very large, which is implied by the reaction rate going to zero (no reaction). Thus, for  $\xi$  small, the above analysis is restricted to a region near the leading edge of the boundary layer. While this is certainly an adequate and logical setup, it does not bring out the essential idea behind the perturbation scheme—that the zero'th order equations hold for the case of chemical equilibrium. It would be much more satisfying to use a small parameter which by definition, tends to zero for the case of chemical equilibrium. This might involve using a chemical time which depends on the net reaction rather than on either the dissociation or recombination reaction alone. These improvements could not be carried out during the present contract period due to the shortness of this period. However, they should be considered in any future work.

#### CALCULATIONS ON THE EXISTENCE OF A BUFFER LAYER

In Ref. 1, the existence of the postulated buffer layer was said to be roughly dependent on the ratio of the characteristic time of recombination compared to the characteristic time of residence (convective or diffusive characteristic times),  $R_z$ . When  $R_z \ll 1$ , then the chemical time is much less

than the residence time and supposedly equilibrium exists. If  $R_t \sim 1$ , then possibly reaction at the wall might exist, and, for  $R_t \gg 1$ , the reaction at the wall certainly exists. In Ref. 1, the time associated with the convection of nitrogen was used. However, if one wishes to take account of the effects of a shock wave, then in order to be consistent one must compare the residence time for the oxygen atoms with the chemical times associated with these atoms, since the change in concentration through the wave means that the residence time associated with the nitrogen may not be close to the time associated with the oxygen atoms. Hence a slightly different  $R_t$  is defined as follows.

$$R_t = \frac{\frac{\rho}{L} k_2}{(2k_n)^2 \left(\frac{P}{P_0}\right)^2 \frac{L}{T^2} \frac{k_2^2}{(k_2+1)}} \quad (27)*$$

This is seen to be the ratio of the mass of oxygen atoms convected per unit volume per unit time to the mass of oxygen atoms disappearing by chemical action per unit volume per unit time, or  $t_c/t_r$ , where  $t_c$  is the characteristic chemical time and  $t_r$  is the characteristic time associated with the convection (i.e., residence time). The expression for  $R_t$  can be calculated if the altitude, Mach number, and  $L$  are given. Since  $L$  is not an aerodynamic parameter, the term  $R_t L$  is plotted versus altitude with Mach number as a parameter in Fig. 1 (dashed lines). The values of temperature, pressure, etc., at the various altitudes were taken from Ref. 5. Thus, if  $L = 1$  foot, and  $M = 11$ , then  $R_t = 1$  at 92,000 feet altitude, and above this altitude a buffer layer could not exist, while below it one could. As in the analysis in Ref. 1., calculations for the dashed curves were made with no shock upstream of the boundary layer and with  $k_2 \sim 1$ .

Next, at the other extreme, the solid curves in Fig. 1 were calculated using the conditions existing behind a normal shock wave at the indicated Mach number and altitude.<sup>6</sup> Comparison of the solid and dashed curves at the same Mach number indicate that the effect of the shock is to reduce the chemical time considerably. This means that the buffer layer would exist at a higher altitude. This effect is dependent on the great change in pressure through a shock wave, the increase causing a faster reaction rate. Also, it should be noted that more realistic values for  $k_2$  were used since the actual values existing behind the shock were available. Of course, even the solid curves can be used only as an indication of the probable values since the actual shocks would be oblique and not normal. For this reason, the curve describing the actual conditions existing on the portion of a vehicle behind the curved nose would probably fall somewhere in between the dashed and solid curves at any given Mach number, but much closer to the solid curves. It should be noted also that the inclusion of a shock wave changes the characteristic of the curves in that the curvature is changed, and more importantly, the variation of  $R_t$  with Mach number at a given altitude is reversed. Without the wave,  $R_t$  increases as the  $M$  increases, while with the wave,  $R_t$  decreases as  $M$  increases. This is no doubt due to the actual  $k_2$  values used in the solid curves. Hence the variation in the solid curves is most probably the correct one.

All the curves in Fig. 1 were calculated with a wall temperature of 1500°K.

It was desired to carry out the above calculations at the nose of a blunt body, near the stagnation point. Also, it was desired to see what changes, if any, were caused in the general boundary-layer equations when a stagnation-point region was considered. Thus, the general conservation equations were transformed to the usual coordinates used in three-dimensional flow, as sketched in Fig. 2. Here,  $X$  is the axial distance parallel to the body surface,  $y$  is the distance perpendicular to the body surface,  $R_b$  is the radius of curvature of the body,  $r$  is the radial distance to a point  $P$  in the flow field, and  $\alpha$  is the angular displacement of the radius  $r$  from a given point. Since, the flow was assumed to be axially symmetric, there was no variation with  $\alpha$  and the equations could be written in terms of  $X$  and  $y$ . Other simplifications arise from the facts that (1) as is customary in such studies,  $y/R_b$  is neglected compared to one because the boundary-layer thickness is assumed small compared to the radius of curvature, and (2)  $X \cong r$  since only the region near the stagnation point is being studied. Finally, it was found that with the assumption that  $\delta \sim \sqrt{\frac{\mu}{\rho a_1}}$ , where  $v_e = a_1 X$  is the external flow velocity, an order-of-magnitude analysis for the stagnation-point boundary layer gave essentially the same equations as those usually used for the flat-plate boundary layer. The above assumptions are suggested by the solutions given for the boundary layer over a flat plate at right angles to the flow. Then  $v_e = a_1 X$  is the potential flow solution and  $\delta \sim \sqrt{\frac{\mu}{\rho a_1}}$  is the boundary-layer solution. However, there still are some questions about the validity of these assumptions being the proper ones at the stagnation point. It is true that their use results in a similarity-type solution for the flow at or near a stagnation point, where the flow parameters are essentially functions of one similarity variable, but this in itself does not imply that therefore the solution is a correct one. No physical evidence proves these conditions to be true as yet, and although the equations which follow are those used by almost every investigator in the field, nevertheless, it would be worthwhile to study the stagnation-point flow basically with the idea of proving or disproving the usual assumptions.

The equation which hold for the above described three-dimensional axially symmetric flow near a stagnation point for a quasi-two-component system are as follows:

$$\begin{aligned}
 a) \quad & \frac{\partial}{\partial x} (\rho u x) + \frac{\partial}{\partial y} (\rho v x) = 0 \\
 b) \quad & \rho u \frac{\partial K_2}{\partial x} + \rho v \frac{\partial K_2}{\partial y} = \frac{\partial}{\partial y} \left( \rho D_{12} \frac{\partial K_2}{\partial y} \right) + m_2 K_2
 \end{aligned} \tag{27}$$

$$c) \quad \rho u \frac{\partial K_3}{\partial x} + \rho v \frac{\partial K_3}{\partial y} = -\frac{\partial}{\partial y} \left( \frac{K_3}{1-K_2} \rho D_{12} \frac{\partial K_2}{\partial y} \right)$$

$$d) \quad \rho u \frac{\partial u}{\partial x} + \rho v \frac{\partial u}{\partial y} = -\frac{\partial P}{\partial x} + \frac{\partial}{\partial y} \left( \mu \frac{\partial u}{\partial y} \right)$$

$$e) \quad \rho u \frac{\partial h}{\partial x} + \rho v \frac{\partial h}{\partial y} = u \frac{\partial P}{\partial x} - \frac{\partial \theta y}{\partial y} + \mu \left( \frac{\partial u}{\partial y} \right)^2$$

$$f) \quad \theta_y = -\frac{\lambda}{c_p} \left\{ \frac{\partial h}{\partial y} - (1-\epsilon) \sum_{i=1}^n h_i \frac{\partial K_i}{\partial y} \right\} \quad (27)$$

$$g) \quad P = \frac{\rho R_0 T}{M}$$

$$h) \quad \bar{M} = \frac{M_1}{1+K_2}$$

It is evident, after seeing Eqs. (27), that since these equations are almost exactly the same as those used in the flat-plate studies, that the same definition could be used for  $R_t$ . That is, one could use a residence time based on the diffusive or convective characteristic times. However, for the case of the blunt body, a somewhat better residence time may be found by using the velocity behind the separated shock, and the distance between the shock and the body. Furthermore, the concentration existing behind the shock at the stagnation streamline may be used since at this point the shock is normal, and the concentrations are known. A sketch of the stagnation-point region with the symbols used is shown in Fig. 3.

According to Li<sup>7</sup>, the detachment distance at  $x=0$ , say  $b$ , is given by the following formula:

$$b = \left\{ \frac{-1 + \sqrt{1 - (1-k)^2}}{(1-k)^2} \right\} k R_{s_0} \quad (28)$$

where  $k = \rho_{\infty} / (\rho_s)_{x=0}$ , the subscript  $s$  denoting conditions immediately behind the shock, and where  $R_{s_0}$  is the radius of curvature of the shock at  $x=0$ . If, as assumed by Li, the radius of curvature of the shock is the same as that of the body, at  $x=0$ , then  $b$  can be calculated.

Next, an order of magnitude of the velocity of the flow between the shock and the body must be found. At the body, the velocity is zero, of course.

Furthermore, according to calculations based on the potential flow around a blunt body, the velocity in the  $y$  direction outside the boundary layer is proportional to  $y$ , i.e.,

$$v_x = -a_1 y \quad (29)$$

and the  $v_x$  velocity in the boundary layer is well approximated by a linear function. Hence the average velocity in the region between the detached shock and the body, along the stagnation streamline, is, to a very good approximation,

$$v_{av} = \frac{v_s}{2} \quad (30)$$

where  $v_s$  is the velocity immediately behind the shock. The residence time in this case is then the time spent in traversing the distance  $b$  along the line  $x=0$ , and is

$$t_r = \frac{b}{v_{av}} \quad (31)$$

The characteristic chemical time consistent with Eq. (31) is then

$$t_c = \frac{(P_2)_s}{(m_2 K_2)} \quad (32)$$

where  $(P_2)_s$  is the partial density of the oxygen atoms behind the shock wave.  $m_2 K_2$  is calculated using the concentrations of  $O$ , and  $O_2$  existing behind a normal shock, but at the temperature of the wall. This is then a very conservative calculation, since the temperature behind the wave is quite high compared to the wall temperature and the reaction rate is therefore considerably higher than at the temperature existing at the wall. However, since no real knowledge of the temperature profile in this region exists, the most conservative value for the temperature, and thus reaction rate, was chosen. Also, again on the conservative side, the wall temperature was chosen the same as for the flat-plate calculations, although the nose temperature would, in general, be considerably higher.

From Eqs. (31) and (32), the time-ratio function,  $R_t$ , can be written as follows:

$$R_t = \frac{t_c}{t_r} = \frac{(P_2)_s}{(m_2 K_2)} \frac{v_{av}}{b} \quad (33)$$

and finally, the function plotted,  $R_t R_{b_0}$ , can be found by substituting for  $b$ ,  $v_{av}$ , and  $m_2 K_2$ . Thus,



$$R_t R_{b_0} = \frac{v_5}{2 \left\{ \frac{-1 + \sqrt{1 - (1-k)^2}}{(1-k)^2} \right\} k} \frac{(K_2)_s}{(2k_p) 2 \left( \frac{P}{P_0} \right)_s^2 \frac{1}{T_w^2} \left[ \frac{K_2^2}{K_2 + 1} \right]_s} \quad (34)$$

Using values given in Ref. 6, the above time-ratio function was calculated and plotted versus altitude with Mach number as a parameter.\* These curves are shown in Fig. 4. It is interesting to note that they have the same curvature as the solid curves in Fig. 1, and fall between the solid and dashed lines of Fig. 1, but closer to the solid lines as expected. For a nose radius of one foot at the stagnation point, these curves show that at a flight Mach number of eleven, the "cross-over point," i.e., that altitude above which there is no buffer layer, but reaction along the wall, is approximately 200,000 feet. If the nose radius is 1/10 feet, then the cross-over altitude drops to 168,000 feet, etc.

The curves of Fig. 4 hold only at or near the stagnation point, and it is desirable to attempt to deduce what occurs as points farther from the stagnation point are considered. First, as  $\chi$  increases, both  $b$  and  $v_5$  increase.  $b$  increases since the shock begins to diverge from a path parallel to the body, and  $v_5$  increases because the shock becomes more oblique to the incoming flow. As a result, it is difficult to ascertain just what does happen to the residence time. However, the pressure decreases also, and since the chemical time depends on the square of the pressure, the chemical characteristic time probably increases so that the result is probably larger  $R_t R_{b_0}$ . That is, from the above arguments, one might expect that as one considers points farther from the stagnation point, the initial effect is an increase in  $R_t R_{b_0}$  and hence a decrease in the cross-over altitude. However, these arguments are not conclusive since, as one moves from the stagnation point, the residence time calculation must be changed because the air no longer impinges on the wall, but is carried along in the boundary layer until it is convected or diffused to the wall. This process takes much longer, and the residence-time calculation used in Fig. 1 must be used. The result of this argument would mean that since the residence time increases considerably, while the pressure would not be very much different from that behind a normal shock, the solid curves in Fig. 1 would hold as one moves away from the stagnation point. However, it is not clear what will happen as a point very far from the stagnation point is considered. While the residence time will be increased due to the boundary-layer effects, the pressure field will be quite changed also, and it is possible that the reaction rate will be slowed enough to cause recombination at the wall again. The shape of the body and hence the shape of the shock must be known to settle this question.

---

\*In this equation, as in others containing the reaction-rate function,  $P_0 = 82.06 \frac{\text{cm}^3 - \text{atmospheres}}{\text{mole} - \text{ox}}$ ,  $P$  is in atmospheres, and  $T_w$  is in °K.

If the above arguments are good for a blunt body, then the curves in Figs. 1 and 4 may be used to predict the approximate distance between the stagnation point and that point on the body where surface reaction ends and a buffer layer begins. As an example, consider a blunt-nosed body with a nose radius of one foot (at  $X = 0$ ), traveling at a Mach number of 11. At an altitude of 200,000 feet,  $R_t R_{b_0} \cong 1$ , and since  $R_{b_0} = 1$  foot,  $R_t = 1$ . Hence, at this altitude, atomic species can reach the wall. In order to find out how far along the nose this atom-wetted area extends, Fig. 1 is used, since away from the stagnation point the boundary layer must be considered. From the solid curves in Fig. 1, if  $M = 11$ , and the altitude is 200,000 feet,  $\angle R_t \cong 0.09$ , or  $R_t = 0.09/L$ . This means that  $R_t \leq 1$  if  $L \geq 0.09$  feet. The curves are used in this manner since Fig. 1 holds only after a boundary layer has been established, and Fig. 4 holds only at or very near the stagnation point.

Admittedly, there is a contradiction involved since, according to Fig. 1, there will always be a surface reaction, if the  $L$  considered, is small enough. However, since Fig. 1 does not hold unless the boundary layer has been well established, and since for very small  $L$ , the stagnation-point calculation holds, it is assumed that no surface reaction will occur at the nose until it has been predicted by the stagnation-point calculation (Fig. 4). This means that if atoms can reach the surface near the stagnation point, they have entered the boundary layer near the body and so then the boundary-layer calculations can be used. This again represents a conservative computation since  $R_t = 1$  in the stagnation-point flow means that the reaction can be completed just as the wall is reached and any atoms swept along the surface by the boundary layer could recombine shortly after entering the boundary layer and thus never reach the body.

It should be emphasized that the above arguments are good only for an order-of-magnitude calculation, and as such, depend very much on the validity of the reaction-rate parameters used. For instance, if the reaction rate proposed by Davidson and used by Fay and Riddell<sup>9</sup> were used, then the results would be considerably different. In the calculations in this report, Hirschfelder's values were used.<sup>10</sup>

#### SIMILARITY BETWEEN DISSOCIATED AND NONDISSOCIATED FLOWS

In Ref. 1, it was mentioned that if a buffer layer existed, as was certainly the case if there was chemical equilibrium, it seemed possible that a similarity between dissociated and nondissociated flows could be found. This would make the calculation of the heat transfer at the wall, for example, much simpler. This similarity argument depended on the possibility of calculating the thickness and the velocity at the edge of the buffer layer. For equilibrium flow, then, it meant finding the boundary-layer variable which formed the edge of the buffer layer, and by a suitable choice of Prandtl number link-

ing the buffer layer to a similar undissociated boundary layer. While this calculation is not necessarily easy to perform, since it involves integrating across the dissociation zone, it would seem to offer the only possibility for similarity in the dissociated boundary layer.

Recently, however, Kuo has published a paper in which similarity is claimed for a boundary layer in equilibrium.<sup>11</sup> His similarity computations do not depend on the existence of a buffer layer, but do involve some rather restrictive assumptions. To improve understanding of the effects of these assumptions, Kuo's method will be used on the equations in the notation of the present report and Ref. 1.

First it should be noted that Kuo, through the assumption illustrated by his Eq. (4.5),  $c_p = \left(\frac{\partial H}{\partial T}\right)_p$ , has deleted a very important term from the energy equation. Thus, in defining  $\bar{c}_p \frac{\partial T}{\partial y}$ , one should really consider the following derivation.

$$h = \sum_i \kappa_i h_i \quad (35)$$

Therefore

$$\begin{aligned} \frac{\partial H}{\partial T} &= \sum_i h_i \frac{\partial \kappa_i}{\partial T} + \sum_i \kappa_i \frac{\partial h_i}{\partial T} \\ &= \sum_i h_i \frac{\partial \kappa_i}{\partial T} + \bar{c}_p \end{aligned} \quad (36)$$

Or, as used in the energy equation,

$$\frac{\partial h}{\partial y} = \sum_i h_i \frac{\partial \kappa_i}{\partial y} + \bar{c}_p \frac{\partial T}{\partial y} \quad (37)$$

At any rate, the term  $\sum_i h_i \frac{\partial \kappa_i}{\partial T}$  is the term deleted by Kuo, and as a result his energy equations has this term multiplied by the Lewis number ( $\mathcal{L}_e$ ) alone, instead of the correct multiplier,  $-(1-\mathcal{L}_e)$ . This multiplier is important because of the obvious implication of  $\mathcal{L}_e = 1$ . Thus, if Kuo's equations are interpreted by replacing  $\mathcal{L}_e$  by  $-(1-\mathcal{L}_e)$ , then the conclusions hold.

Equation (45e) in Ref. 1 most closely resembles Kuo's Eq. (5.6). The similarity is exact if  $\frac{\partial \psi}{\partial \eta}$  and  $-\frac{\partial \psi}{\partial \xi}$  are interpreted as  $u$  and  $v$  in Kuo's paper. Equation (45e) is repeated here for reference.

$$u \frac{\partial h}{\partial x} + v \frac{\partial h}{\partial y} = \nu_e \frac{\partial}{\partial y} \left[ \frac{c}{R} \left\{ \frac{\partial h}{\partial y} - (1-\mathcal{L}_e) \sum_i h_i \frac{\partial \kappa_i}{\partial y} \right\} \right] + \nu_e \left( \frac{\partial u}{\partial y} \right)^2 \quad (38)$$

Now,

$$\sum_i h_i \frac{\partial \kappa_i}{\partial y} = (h_1 - h_2) \frac{\partial \kappa}{\partial y} \quad (39)$$

since  $h_1 \approx h_3$  and  $\kappa_1 + \kappa_3 = 1 - \kappa_2 = \kappa$ . Furthermore,

$$\begin{aligned} \frac{\partial \kappa}{\partial y} &= \frac{\partial \kappa}{\partial T} \frac{\partial T}{\partial y} + \frac{\partial \kappa}{\partial P} \frac{\partial P}{\partial y} \\ &= \frac{\partial \kappa}{\partial T} \frac{\partial T}{\partial y} \end{aligned} \quad (40)$$

since in the boundary layer  $\frac{\partial P}{\partial y} \approx 0$ . Therefore,

$$\sum_i h_i \frac{\partial \kappa_i}{\partial y} = \frac{(h_1 - h_2)}{\bar{c}_p} \left( \frac{\partial \kappa}{\partial T} \right)_P \bar{c}_p \frac{\partial T}{\partial y} \quad (41)$$

Finally, substituting for  $\bar{c}_p \frac{\partial T}{\partial y}$  from Eq. (37) and solving for  $\sum_i h_i \frac{\partial \kappa_i}{\partial y}$  one obtains the following relation.

$$\sum_i h_i \frac{\partial \kappa_i}{\partial y} = \frac{\partial h}{\partial y} \left\{ \frac{\frac{(h_1 - h_2)}{\bar{c}_p} \left( \frac{\partial \kappa}{\partial T} \right)_P}{1 + \frac{(h_1 - h_2)}{\bar{c}_p} \left( \frac{\partial \kappa}{\partial T} \right)_P} \right\} \quad (42)$$

and Eq. (38) becomes

$$\begin{aligned} u \frac{\partial h}{\partial x} + v \frac{\partial h}{\partial y} &= \nu_e \frac{\partial}{\partial y} \left[ \frac{C}{R} \frac{\partial h}{\partial y} \left\{ 1 - (1 - Le) \frac{(h_1 - h_2)}{\bar{c}_p} \left( \frac{\partial \kappa}{\partial T} \right)_P \frac{1}{\left( 1 + \frac{(h_1 - h_2)}{\bar{c}_p} \left( \frac{\partial \kappa}{\partial T} \right)_P \right)} \right\} \right] \\ &\quad + \nu_e \left( \frac{\partial u}{\partial y} \right)^2 \end{aligned} \quad (43)$$

Now as Kuo points out, Eq. (43) is exactly that equation which holds for undissociated flow if  $C = \text{constant}$ , and if one considers this undissociated flow to have a Prandtl number of  $R/\sigma$  where  $R$  is the dissociated flow Prandtl number and  $\sigma$  is the term in the brackets, i.e.,

$$\sigma = 1 - (1 - \mathcal{L}e) \frac{(h_1 - h_2) \left( \frac{\partial K}{\partial T} \right)_p}{\bar{c}_p} \frac{1}{\left( 1 + \frac{(h_1 - h_2) \left( \frac{\partial K}{\partial T} \right)_p}{\bar{c}_p} \right)} \quad (44)$$

and is constant. It should be noted that the above equation differs from Kuo's in two respects. First, the term  $1 - \mathcal{L}e$  is included, and thus illustrates that for  $\mathcal{L}e = 1$ , the similarity is exact with no extra assumption. Secondly, in Kuo's paper  $\left( \frac{\partial K}{\partial T} \right)_p$  has been calculated from the dissociation reaction, in terms of  $\mathcal{E}$ , a parameter which measures the amount of mass reacted. Insofar as  $\sigma$  being constant is concerned,  $h_1 - h_2$ , as well as  $\bar{c}_p$  can be assumed constant with some degree of accuracy, but it is not clear that  $\left( \frac{\partial K}{\partial T} \right)_p$  is a constant. According to Kuo,  $\sigma$  changes very little with temperature, but he used only values for nitrogen at relatively low temperatures (5000°K to 8000°K) where one would expect the amount of nitrogen dissociated to be small compared to the amount of oxygen dissociated. In fact, the oxygen dissociation is the main consideration at these temperatures and should certainly be used instead of the nitrogen dissociation. For this reason, it is still not clear whether the assumption that  $\sigma = \text{constant}$  is a good one to make.

#### EXPERIMENTAL FACILITIES

In Ref. 1, a number of methods for obtaining hypersonic flow was discussed. As indicated in that discussion, most methods employed in the experimental investigation of hypersonic flow fall short of obtaining high stagnation temperatures and pressures at high Mach numbers. Although appropriate for some specific areas of investigations, they are limited insofar as simulation of actual hypersonic flight conditions are concerned. Full simulation would have the advantage of determining the significant parameters for obtaining the information of interest. It would also provide a means for testing the current theories predicting significant parameters and the regions of their validity.

The wind-tunnel with pebble heater for increasing the stagnation temperature is limited in temperatures obtainable and therefore also limited in the Mach numbers which can be reached. In the helium tunnel, temperatures are extremely low and "real gas" effects are eliminated. The firing of pellets has proven somewhat successful for some measurements but instrumentation becomes difficult especially in the case of boundary layer measurements. High temperatures are obtained in a conventional shock tube but only relatively low Mach numbers are possible. Modifications of the shock tube are possible for hypersonic flow, however.

Infinitely high Mach numbers can theoretically be obtained in a shock tube in the region between the contact surface or interface and the expansion wave. This occurs through a nonsteady isentropic expansion through which stagnation temperature increases. High Mach numbers in this region have not been obtained experimentally but a possible explanation may be the imperfect diaphragm rupturing, which might be corrected by proper diaphragm design. The desired testing conditions of high temperatures and pressures as well as high Mach number are obtainable, according to theory, using a detonation wave as a driver so that not only is a high temperature initially obtained, in the reservoir gas, but also advantage is taken of the convective force of detonation. Of course, this would mean testing in the detonation gases, unless two diaphragms are employed with air in the section between the two diaphragms, heated by the detonation gases in the section behind the first diaphragm. However, the testing time available is the time between the arrival of the contact surface in the test section and the arrival of the tail of the expansion wave. Since the contact surface travels with the velocity of the fluid and the expansion wave travels with the local velocity of sound relative to the fluid, the testing time available per foot of tube length, for a given test-section temperature, becomes approximately inversely proportional to the test Mach number squared—or very small at high Mach numbers ( $\sim 4 \frac{\mu \text{ sec}}{\text{ft}}$  at  $M = 15$ ).

The detonation wave might be used in another way. Since temperatures of  $4500^\circ\text{K}$  and pressures of 40,000 psi have been obtained behind a detonation wave, it would be possible to obtain stagnation temperature and pressure of the order desired by reflecting a detonation wave and expanding the stagnation gas through a nozzle. Aside from the severe structural problems, this method has the disadvantage of requiring testing in the combustion gases instead of air.

A different approach is to increase the Mach number of flow available for testing in a conventional shock tube in the region between shock and interface by the addition of an expansion nozzle to the low-pressure region. With this modification, however, there are several limitations to achieving the hypersonic conditions of interest. For the limited high pressure in the reservoir obtainable by usual methods, the pressure and density in the test region are very low at high test-chamber Mach numbers. In order to obtain higher densities at high Mach numbers, extremely high energies are required initially in the reservoir gas. Assuming the air will be in chemical equilibrium, the energy required for the stagnation conditions necessary for isentropic expansion to the required testing conditions can be estimated from tables not available. The problem becomes one of how to transfer such extremely large quantities of energy to the reservoir air.

The use of electrical energy has proven to be a method by which very high reservoir temperatures and pressures are obtainable. In general, electrical energy provides the most versatile method for a large variety of operating conditions. It is easily controllable. There is no warm-up or cooling-off period. There is immediate response to external control. A minimum or space is required in the wind-tunnel area.

The general approach is to store the energy required at a relatively slow rate for withdrawal over a very short period of time through an arc. This can be done in several ways. At Tullahoma (AEDC), a condenser bank has been em-

ployed as the source of electrical energy. Such an arrangement has many disadvantages. It is extremely costly and establishment of proper safety conditions is difficult. There is also an inordinate space requirement for the installation of condenser banks.

The inductive method for energy storage has definite advantages when millions of watt-sec are to be stored. Early and Walker<sup>12</sup> have studied the problem of obtaining tremendous energy over a period of a few milliseconds. They have built and tested an induction coil with the necessary switching arrangements developed for the purpose. Important advantages of this approach for high-energy installation are economy, safety, and relatively small space requirements.

Large currents are required for charging the coil. One source of d-c power advantageous for charging purposes is the unipolar generator. Such a generator can be constructed to deliver over 100,000 amperes. Allis Chalmers has developed a high-current unipolar generator which makes use of a fly wheel and can deliver  $\sim 7 \times 10^7$  joules. This generator, however, is still extremely expensive and requires expensive auxiliary equipment. A much more simple and economical power supply is the ignitron rectifier designed to make maximum use of the line power available in conjunction with a transformer type of coil. A major consideration here is the power available off the utility line.

The arc discharge tunnel has many advantages not the least of which is the fact that theoretically it has no limitations as to Mach number, test conditions or run time. Of course practically there are many limitations. As energy requirements increase the tremendous cost of power plants becomes a problem. As Mach numbers increase for a reasonable pressure in the test chamber, a high stagnation pressure is required. This has already become a problem in the design of new tunnels. Pressure vessels for 300,000 psi have not yet been designed or built. Yet pressures greater than this would be required to simulate high Mach number flow at approximately 50,000 feet altitude.

A number of problems arise in the design of the arc discharge tunnel. Since it is essentially a blow-down arrangement, the reservoir has to be large enough and/or the throat small enough so that the outflow of gas does not change the reservoir conditions so rapidly that testing time is cut short as a result. But the smaller the throat size, the greater the change in Mach number during a run, as a result of throat erosion by the hot gas. Of course, the larger the reservoir, the greater the total energy required to raise the air to the necessary stagnation conditions. This means the size of the reservoir is determined by the throat size as well as the amount of energy transferable to the reservoir gas. Or conversely, the energy required is determined not only by the stagnation conditions but also by throat size, which, of course, is in turn determined by test-section size.

The efficiency of energy transfer from the arc to the air may change radically with initial density, although at high initial densities there seems to be some evidence to the contrary. There is also some question as to what is the expansion process through the nozzle. At such high temperatures there are high heat losses in the throat region as well as in the reservoir. Although the flow through the downstream section of the nozzle may be isentropic, there is some doubt as to what occurs in the region of the throat. Computations are also difficult due to the lack of extensive tables for "real gas" properties. Approximations can be made based on ideal gas parameters, but these can be incorrect by extremely large factors. Even ideal gas functions are not available for the high density region.

Design conditions can be approximated by assuming an equilibrium mixture of ideal gases and a quasi-steady-state process. The energy necessary to raise the temperature of  $\sim .05$  cubic feet of air at a density of  $\sim 100$  times standard to  $7000^\circ\text{K}$  is  $\sim 2 \times 10^6$  joules (The total energy required to raise the same volume of reservoir gas to a given temperature is less at lower densities, even though the internal energy of equilibrium air increases with decreasing density and pressure at a given temperature.) Assuming a specific heat ratio of 1.4, for a .01-foot-diameter throat, the reservoir density will decrease 10 percent in  $\sim 15$  milliseconds. This time increases for a decrease in constant specific heat ratio. If only 25 percent of the energy in the coil enters the air, with a coil storage of  $\sim 8 \times 10^6$  joules, a test-chamber density of  $\sim .01$  times standard at a Mach number of  $\sim 15$  can be obtained, with a run time of about 15 milliseconds. This relatively high density and run time make measurements of all kinds very much easier than measurements in the ordinary shock tunnel where test-chamber densities are low and run times are less than a millisecond.



REFERENCES

1. Adamson, T. C., Jr., Nicholls, J. A., and Sherman, P. M., A Study of the Hypersonic Laminar Boundary Layer with Dissociation, Engineering Research Institute Report No. 2606-6-T, The University of Michigan, May, 1957.
2. Probststein, Ronald F., The Effect of Variable Fluid Properties on the Equilibrium Laminar Boundary Layer Surface Heat Transfer Rate at Hypersonic Flight Speeds, WADC Tech. Note 56-2, December, 1955.
3. Hansen, C. F., "Note on the Prandtl Number for Dissociated Air," Journ. Aero. Sci., 20 (Nov., 1953), 789-790.
4. Marble, F. E., and Adamson, T. C., Jr., "Ignition and Combustion in a Laminar Mixing Zone," Jet Propulsion, 24 (March-April, 1954), 85-94.
5. The Standard Atmosphere Sea Level to 300,000 Feet, Bell Aircraft Information Note No. 3, June, 1956.
6. McKowen, P., The Equilibrium Composition and Flow Variables for Air Dissociated by a Strong Shock Wave, Bell Aircraft Report No. 02-984-040, March 8, 1957.
7. Li, T. Y., and Geiger, R. E., "Stagnation Point of a Blunt Body in Hypersonic Flow," Journ. Aero. Sci., 24 (Jan., 1957), 25-32.
8. Schlichting, H., Boundary Layer Theory (McGraw-Hill Book Co., Inc., New York, 1955), pp. 70-75.
9. Fay, J. A., and Riddell, F. R., Theory of Stagnation Point Heat Transfer in Dissociated Air, AVCO Research Laboratory, Research Report 1, June, 1956, Revised April, 1957, p. 22.
10. Hirschfelder, J. O., Heat Transfer in a Chemically Reacting Gas Mixture, University of Wisconsin, WIS.-ONR-18, Feb. 6, 1956, p. 15.
11. Kuo, Y. H., "Dissociation Effects in Hypersonic Viscous Flow," Journ. Aero. Sci., 24 (May, 1957), 345-350.
12. Early, H. C., and Walker, R. C., "The Economics of Multimillion Watt-Second Inductive Energy Storage," presented at AIEE Winter Meeting, Jan., 1956.

TABLE I

PERFECT GAS SPECIFIC HEATS OF ATOMIC AND MOLECULAR OXYGEN  
AND MOLECULAR NITROGEN AS A FUNCTION OF TEMPERATURE

T	$C_{P_{O_2}}$	$C_{P_O}$	$C_{P_{N_2}}$
1000	0.260	0.313	0.279
1500	0.273	0.312	0.297
2000	0.282	0.311	0.307
2500	0.291	0.312	0.312
3000	0.298	0.313	0.316
3500	0.305	0.316	0.318
4000	0.311	0.318	0.320
4500	0.314	0.322	0.322
5000	0.317	0.325	0.324

Note: T is in °K

$C_P$  is in cal/gm-°K

Original values of  $C_P/R$  from National Bureau of Standards, Circular 564, Tables of Thermal Properties of Gases.

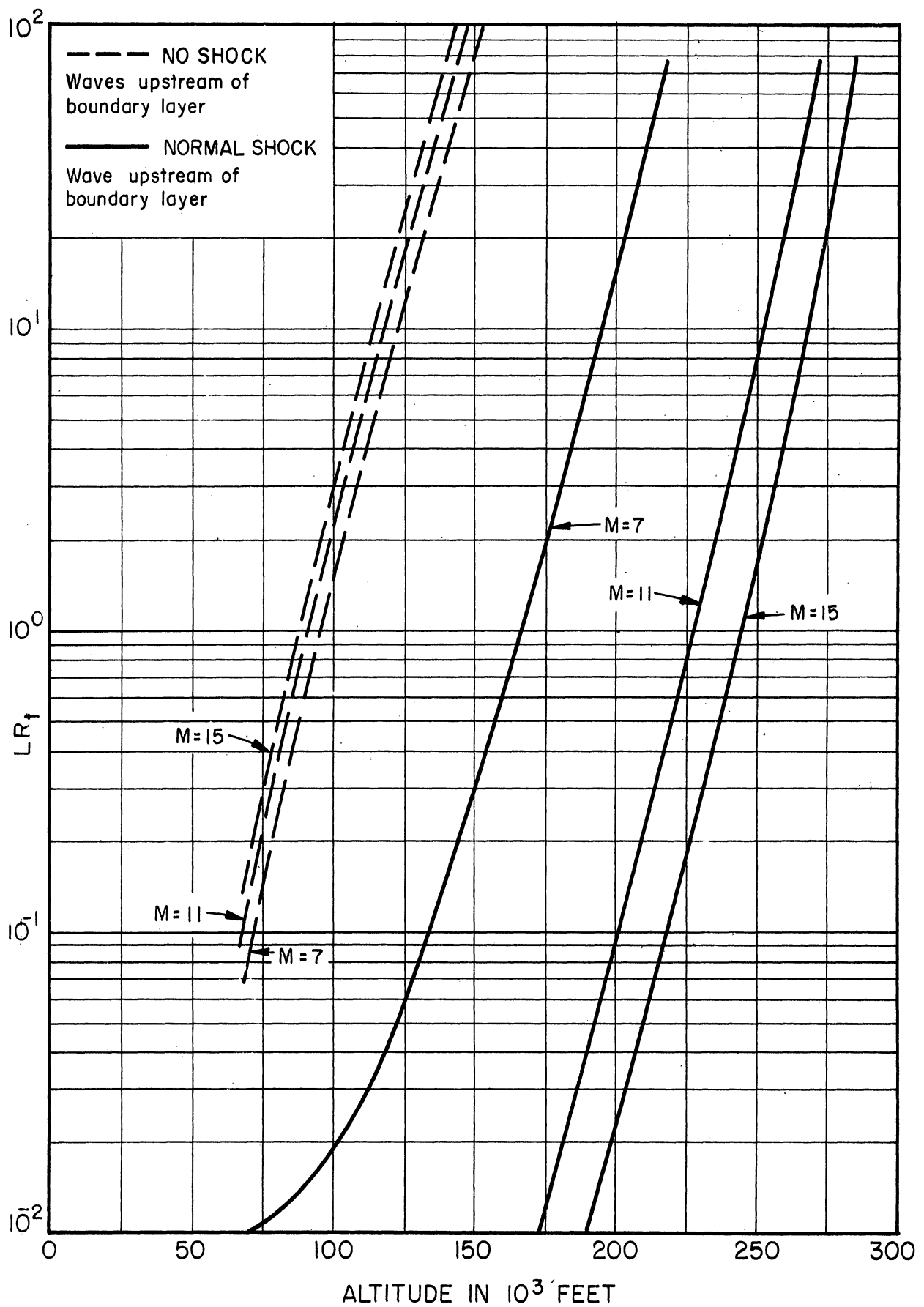


Fig. 1. Variation of time-ratio function with altitude with flight Mach number as parameter for flat plate of length  $L$ . ( $L$  in feet,  $T_w = 1500^\circ\text{K}$ )

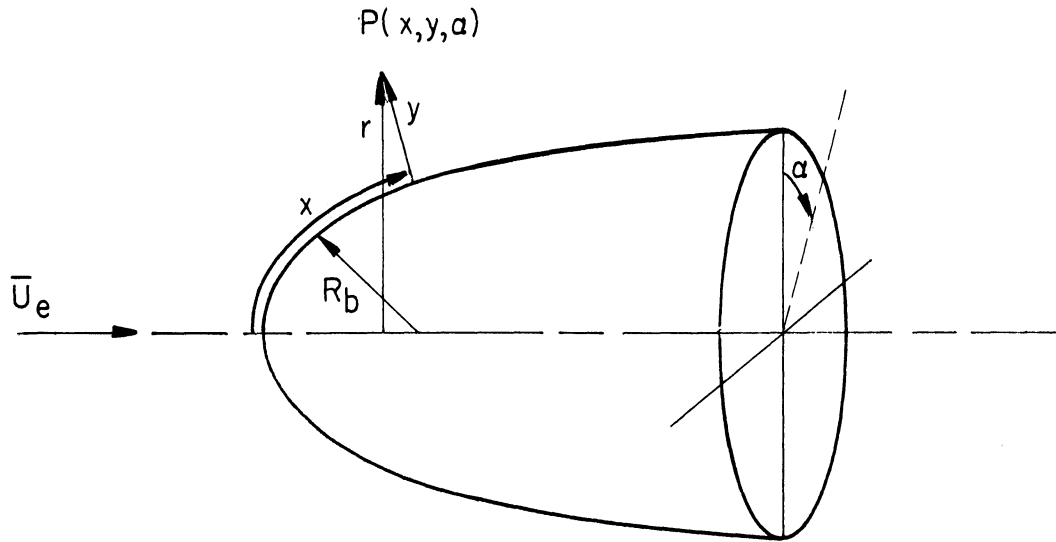


Fig. 2. Three-dimensional coordinates.

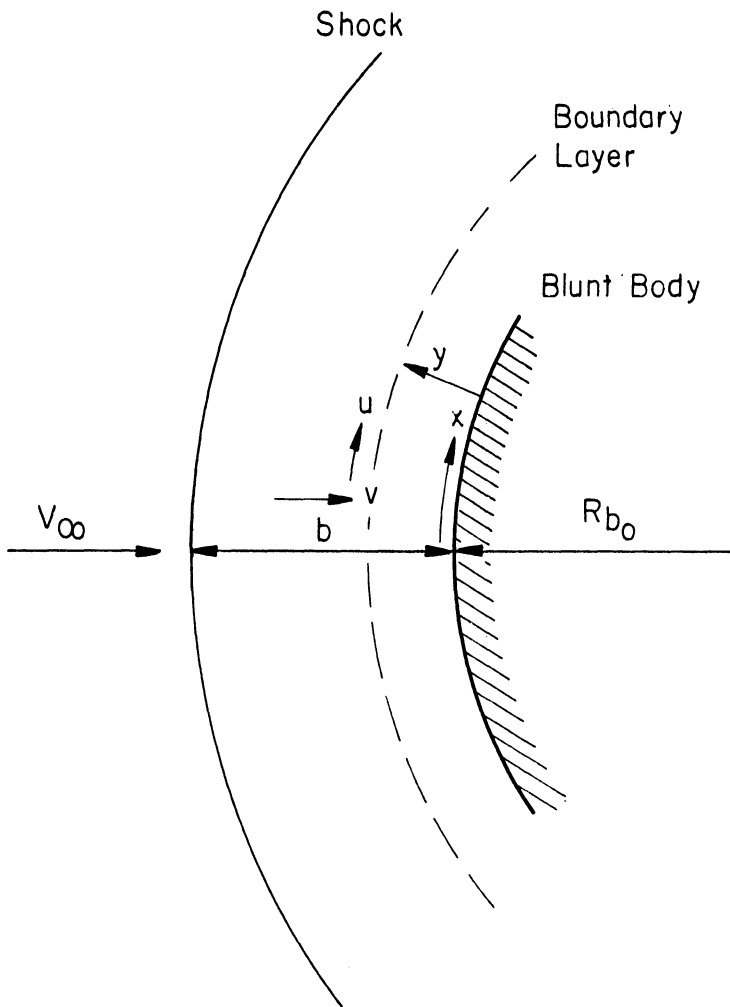


Fig. 3. Stagnation-point region between a detached shock and a blunt body.

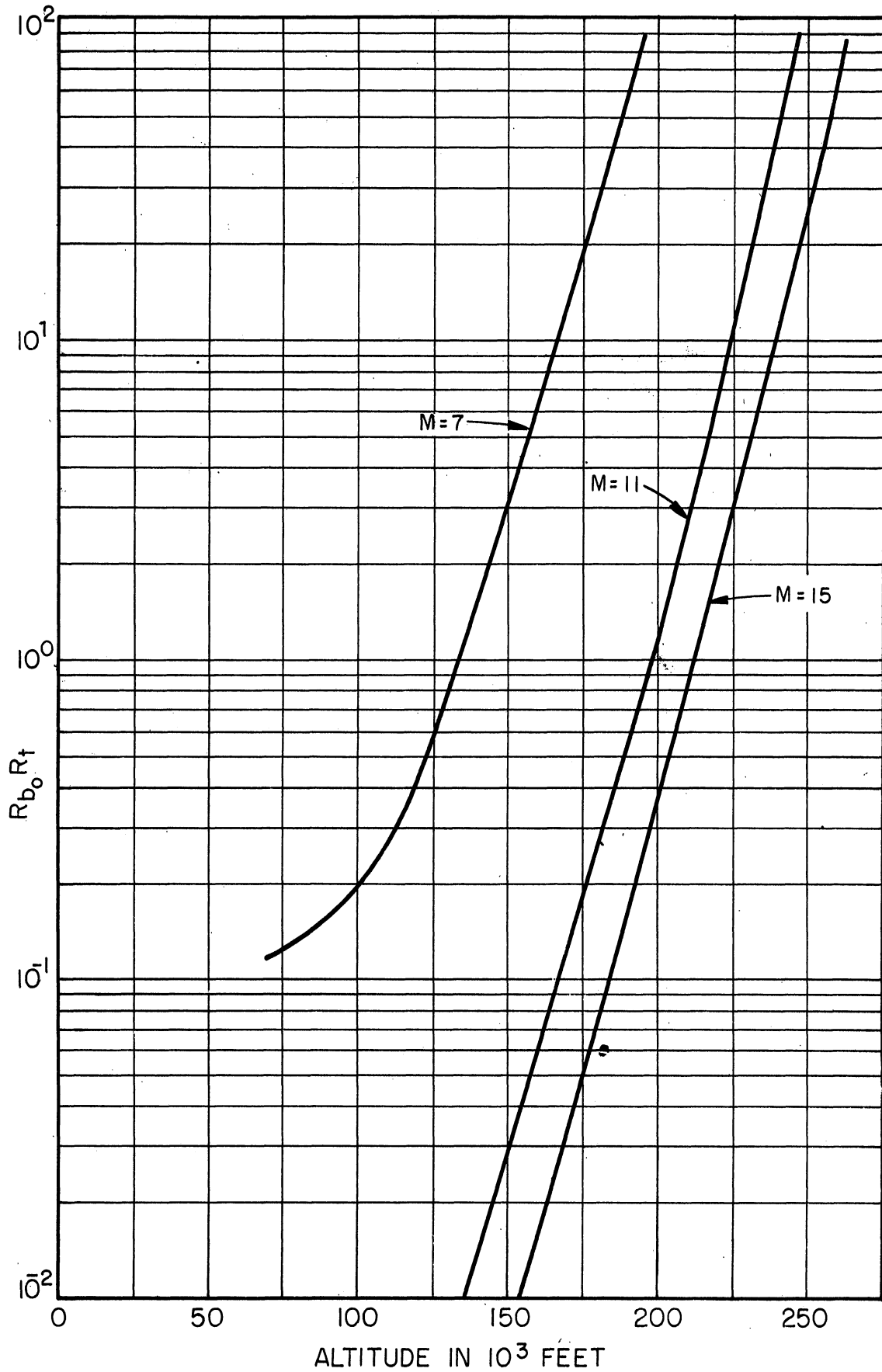


Fig. 4. Variation of time-ratio function with altitude with flight Mach number as parameter for blunt-nose body with radius of curvature  $R_{b_0}$ . ( $R_{b_0}$  in feet,  $T_w = 1500^\circ\text{K}$ )

UNIVERSITY OF MICHIGAN



3 9015 02493 1175